

Effect of gravity modulation on the stability of convection in a vertical slot

By WEN-YAU CHEN AND C. F. CHEN

Department of Aerospace and Mechanical Engineering,
The University of Arizona, Tucson, AZ 85721, USA

(Received 7 January 1998 and in revised form 17 May 1999)

The nature of instability occurring in a differentially heated infinite slot under steady gravity depends only on the Prandtl number of the contained Boussinesq fluid. For fluids with $Pr < 12.5$, the instability is shear dominated and onsets in a steady convection mode; for fluids with $Pr > 12.5$, the instability is buoyancy dominated and onsets in an oscillatory mode. In this paper, we examine the effect of gravity modulation on the stability characteristics of convection in an infinite slot with both kinds of fluids, in particular, $Pr = 1$ and $Pr = 25$. Using the method of Sinha & Wu (1991), we are able to obtain accurate results without excessive numerical integration in the linear stability analysis by Floquet theory. Results show that, for $Pr = 1$, at a non-dimensional oscillation frequency $\omega = 20$, the critical state alternates between the synchronous and subharmonic modes. At higher frequencies, $\omega > 100$, all critical states occur in the synchronous mode. For $Pr = 25$, with a modulation amplitude ratio of 0.5, resonant interaction occurs in the neighbourhood of $\omega = 2\sigma_c$, where σ_c is the oscillation frequency of the instability at the critical state under steady gravity. This resonant interaction is destabilizing, with the critical Grashof number being reduced by approximately 20% from that at steady gravity. It is due to the presence of a detached subharmonic branch of the marginal stability curve. In frequency ranges where the detached subharmonic branch is absent, the critical state is in the quasi-periodic mode consisting of two waves of different oscillation frequencies whose sum is the forcing frequency. An analysis of the rate of change of the perturbation kinetic energy shows that, for $Pr = 1$, the instability is shear dominated regardless of the mode of oscillation, synchronous or subharmonic. Similarly, for $Pr = 25$, the instability is buoyancy dominated whether it is in the quasi-periodic or subharmonic mode. The mode switching is a response to the forcing and is independent of the dominant mechanisms of instability.

1. Introduction

An inverted pendulum can be stabilized by oscillating the pivot in the vertical direction with suitable frequency and amplitude. By the same physical process, the density inversion in a horizontal fluid layer heated from below can likewise be stabilized by vertical oscillation of the layer at suitable frequency and amplitude. This result was obtained through the use of linear stability theory by Gresho & Sani (1970), who first noted the analogy, and by Gershuni, Zhukhovitskii & Iurkov (1970). Gresho & Sani showed that the instability may be in the synchronous or subharmonic mode and that substantial stabilization can be obtained. Biringen & Peltier (1990) investigated the three-dimensional Rayleigh–Bénard problem under gravity modulation by

numerical solution of the full Navier–Stokes equation. For a case predicted to be stable by Gresho & Sani at a Rayleigh number of 4500, they showed that any initial perturbations in the velocity amplitude vanished in a short time.

Saunders *et al.* (1992) studied the effect of gravity modulation on the stability of a double-diffusive layer with stress-free boundaries in both the finger and diffusive cases. They presented stability boundaries in the plane spanned by amplitude and the inverse of modulation frequency for a number of examples. Terrones & Chen (1993) extended the stability study to double-diffusive layers with cross-diffusion including rigid boundaries. A striking feature they found in a double-diffusive layer of low Prandtl number (10^{-2}) fluid is the existence of bifurcating neutral curves with double minima, one of which corresponds to a quasi-periodic asymptotically stable branch and the other to a subharmonic neutral solution. As a consequence, a temporally and spatially quasi-periodic bifurcation from the basic state is possible, in which case there are two incommensurate critical wavenumbers at two incommensurate onset frequencies at the same Rayleigh number. With the presence of cross-diffusion, the subharmonic and the quasi-periodic neutral curves become disconnected.

Convection in an infinite vertical slot has attracted a number of investigators because it offers a relatively simple basic flow to study the instability phenomenon encountered in more practical problems. A brief summary of earlier results was presented by Thangam & Chen (1986), and a more comprehensive review can be found in Chen & Pearlstein (1989). Convection in a fluid contained within an infinite slot with differentially heated walls consists of parallel flows up along the hot wall and down along the cold wall. When the temperature differences across the slot, ΔT , exceeds the critical value, the convection flow becomes unstable. If the Prandtl number, Pr , of the fluid is less than ~ 12.5 , the instability onsets as steady convection rolls in a vertical array. If $Pr > 12.5$, the initial onset is in the oscillatory mode. For the small Pr case, the instability arises in the shear flow generated by buoyancy. At higher Prandtl numbers, the diminished influence of the thermal diffusivity allows the potential energy caused by buoyancy to be transferred into perturbations. This oscillatory instability eventually grows into convection cells, as observed experimentally by Vest & Arpaci (1969) and Chen & Thangam (1985) in high aspect ratio tanks.

Baxi, Arpaci & Vest (1974) were the first to study the effect of gravity modulation on the stability of convection in a vertical slot by linear stability analysis using the Floquet theory. They studied cases with the non-dimensional modulation frequency $\omega \geq 100$. They found, as in a horizontal layer, that convection can either be stabilized or destabilized in different parametric ranges of the modulation frequency and amplitude. Gershuni & Zhukhovitskii (1981) studied the problem under high-frequency gravity modulation with zero mean in any arbitrary direction. The linear stability problem was solved using the method of averaging. Sharifulin (1983) extended the problem to include a non-zero mean but confined the gravity to be in the longitudinal direction of the slot containing fluids with $0 \leq Pr \leq 10$. His conclusion is that high-frequency modulation destabilizes the flow. Recently, Farooq & Homsy (1996) considered the effect of gravity modulation on the linear and nonlinear convection in a slot. The slot is differentially heated with a constant vertical temperature gradient to better approximate the conditions in a finite slot of high aspect ratio. Besides the steady and oscillating modes found in an infinite slot, there is one additional internal wave mode associated with the initial stratification. At small modulation amplitudes, resonant interaction occurs when the modulation frequency matches that of the natural modes of the system. When the modulation amplitude is of the same order as the mean gravity, the parallel-flow modes can be destabilized by the oscillation.

In this paper, we examine the stability characteristics of slot convection under gravity modulation at frequency $\omega = 20$ by linear stability analysis. We note that previous stability studies of this problem were carried out at higher frequency ranges, $\omega > 100$. By applying the method of Sinha & Wu (1991), we are able to obtain accurate results for the eigenvalues without excessive numerical integration. In particular, we examine the effect of gravity modulation on fluids in which instability onsets in a steady convection mode ($Pr = 1 < 12.5$) or in an oscillatory mode ($Pr = 25 > 12.5$) under steady gravity.

Aside from their having different characteristics at the onset of instability, the choice of fluids with $Pr = 1$ and 25 was made with practical considerations for possible experimental investigations in mind. $Pr = 1$ is for air, and we have extensive numerical simulation results of its behaviour under gravity modulation (Jin & Chen 1997). $Pr = 25$ is of similar magnitude to several commonly available fluids or fluid mixtures, such as ethanol ($Pr = 17$) and 30 wt% glycerol–water solution ($Pr = 26$).

In the following, the basic state and the linear stability equations are presented in §2. The method of solution by the Floquet theory and the use of the Chebyshev expansion for calculating the results are briefly explained in §3, along with all the terms comprising the time rate of change of the perturbation kinetic energy in §4. Results for $Pr = 1$ and 25 are discussed in §5, and conclusions are presented in §6.

2. The basic state and the stability equations

Consider two-dimensional fluid motion in an infinite vertical slot of width H whose vertical sides are maintained at different constant temperatures. The gravity vector is pointing downward, and its magnitude oscillates with amplitude g_1 and frequency Ω about a mean g_0 :

$$g = g_0 + g_1 \cos \Omega t. \quad (1)$$

Let the origin of the x, y coordinate system be at the midplane of the slot. The density of the fluid is assumed to be linear with temperature,

$$\rho = \rho_0[1 - \alpha(T - T_0)] \quad \text{with} \quad \alpha = -\frac{1}{\rho} \frac{\partial \rho}{\partial T}. \quad (2)$$

All other thermal physical properties are assumed to be constant. The equations of motion and energy, with the Boussinesq assumption, are rendered non-dimensional by the characteristic length H , time H^2/ν , temperature ΔT , and velocity ν/H in which ν is the kinematic viscosity and ΔT is the temperature difference across the slot.

For the basic state in which the only non-zero component of the velocity is in the vertical direction, $W(x, t)$, and the temperature T is independent of z and linear in x ,

$$T_0 = -x, \quad (3)$$

the non-dimensional momentum equation reduces to

$$\frac{\partial W}{\partial t} = -G_0 x - G_1 x \cos \omega t + \frac{\partial^2 W}{\partial x^2} \quad (4)$$

in which ω is the non-dimensional oscillation frequency and the Grashof numbers G_0 and G_1 are based on g_0 and g_1 , respectively,

$$G_0 = g_0 \alpha \Delta T H^3 / \nu^2, \quad (5)$$

$$G_1 = G_0 g_1 / g_0. \quad (6)$$

The boundary conditions are $W = 0$ at $x = \pm \frac{1}{2}$. The velocity field for the basic flow is

$$W_0(x, t) = W_{01}(x) + W_{02}(x, t) \\ = \frac{G_0}{6} \left(x^3 - \frac{x}{4} \right) + \frac{G_1}{\omega} \left\{ -x \sin \omega t + \frac{N_1(x) \sin \omega t + N_2(x) \cos \omega t}{2 \sinh^2 \lambda \cos^2 \lambda + \sin^2 \lambda \cosh^2 \lambda} \right\} \quad (7)$$

in which

$$\left. \begin{aligned} N_1(x) &= (\cos \lambda \sinh \lambda) \cos 2\lambda x \sinh 2\lambda x + (\sin \lambda \cosh \lambda) \sin 2\lambda x \cosh 2\lambda x, \\ N_2(x) &= (\cos \lambda \sinh \lambda) \sin 2\lambda x \cosh 2\lambda x - (\sin \lambda \cosh \lambda) \cos 2\lambda x \sinh 2\lambda x, \\ \lambda &= (\omega/8)^{1/2}. \end{aligned} \right\} \quad (8)$$

The steady part of the basic velocity is the familiar cubic distribution with the maximum value of $|W_{01}/G_0| = (72\sqrt{3})^{-1} = 8.02 \times 10^{-3}$. The unsteady part is inversely proportional to ω and its magnitude is antisymmetric with respect to $\omega t = \pi$. In figure 1, we show the distribution of $W_{02}(x, t)/G_1$ for $\omega = 20$ during the half-cycle $0 \leq \omega t \leq \pi$. It is seen that the maximum magnitude reaches $\sim 7.0 \times 10^{-3}$. We anticipate that gravity modulation can have important effects on the stability of the flow as g_1/g_0 approaches 1 and $\omega \leq 20$.

In a steady gravity field, natural convection in the slot becomes unstable as G_0 becomes large and the instability takes the form of a vertical array of convection cells (Vest & Arpaci 1969; Hart 1971). Accordingly, we investigate the stability of convection in a gravity-modulated fluid assuming all perturbations are periodic in z , e.g.

$$\left. \begin{aligned} u'(x, z, t) &= \tilde{u}(x, t)e^{ikz}, & w'(x, z, t) &= \tilde{w}(x, t)e^{ikz}, \\ T'(x, z, t) &= \tilde{T}(x, t)e^{ikz}, & p'(x, z, t) &= \tilde{p}(x, t)e^{ikz}. \end{aligned} \right\} \quad (9)$$

When these quantities are substituted into the basic equations and the nonlinear terms are neglected, we obtain the following linear stability equations in which the tilde has been dropped:

$$\frac{\partial}{\partial t} (D^2 - k^2) \Psi - ik[\Psi D^2 W_0 - W_0(D^2 - k^2) \Psi] - (D^2 - k^2)^2 \Psi \\ = - (G_0 + G_1 \cos \omega t) DT, \quad (10)$$

$$\frac{\partial T}{\partial t} + ik(W_0 T - \Psi) = \frac{1}{Pr} (D^2 - k^2) T. \quad (11)$$

In these equations, $D = d/dx$, $Pr = \nu/\kappa$, with κ the thermal diffusivity, and Ψ is the perturbation stream function,

$$u = ik\Psi \quad \text{and} \quad w = -D\Psi. \quad (12)$$

The boundary conditions at $x = \pm \frac{1}{2}$ at any t are

$$\Psi = D\Psi = T = 0. \quad (13)$$

3. Method of solution

We use the Galerkin method for the stability analysis. The perturbation quantities Ψ and T are expanded into their respective trial functions, Ψ_n and T_n :

$$\Psi(x, t) = \sum_{n=1}^N a_n(t) \Psi_n(x), \quad T(x, t) = \sum_{n=1}^n b_n(t) T_n(x), \quad (14)$$

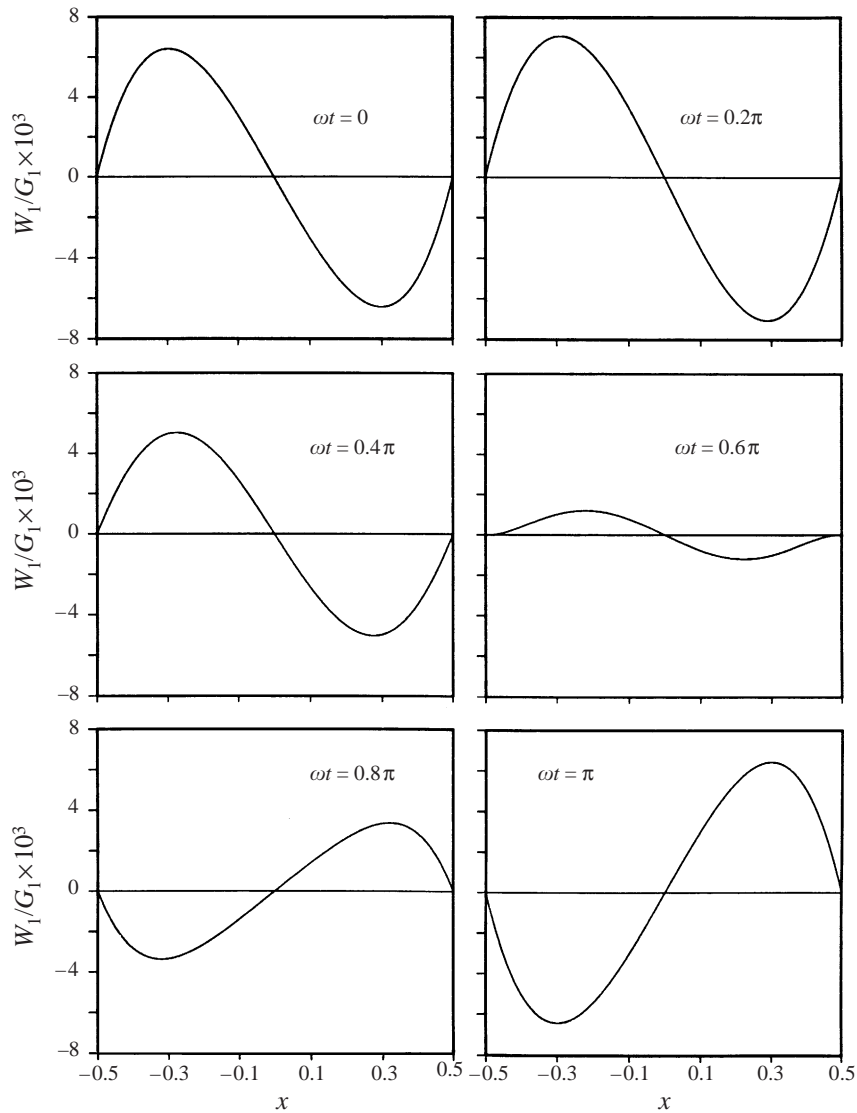


FIGURE 1. Oscillatory part of the basic velocity distribution in the slot at $\omega = 20$ for $0 \leq \omega t \leq \pi$.

with $\Psi_n(x)$ the Chandrasekhar (1961) functions and T_n the trigonometric functions:

$$\Psi_n(x) = \begin{cases} \frac{\cosh(\rho_n x)}{\cosh(\rho_n/2)} - \frac{\cos(\rho_n x)}{\cos(\rho_n/2)} & \text{where } \tanh(\rho_n/2) + \tan(\rho_n/2) = 0 \text{ if } n \text{ odd} \\ \frac{\sinh(\mu_n x)}{\sinh(\mu_n/2)} - \frac{\sin(\mu_n x)}{\sin(\mu_n/2)} & \text{where } \coth(\mu_n/2) - \cot(\mu_n/2) = 0 \text{ if } n \text{ even,} \end{cases} \quad (15)$$

$$T_n x = \begin{cases} \cos n\pi x, & n \text{ odd} \\ \sin n\pi x, & n \text{ even.} \end{cases} \quad (16)$$

When the truncated series expansions, (14), are substituted into (10) and (11) and

the Galerkin operations are performed with unity weighing function, we obtain

$$\frac{d}{dt} \begin{Bmatrix} a_i \\ b_i \end{Bmatrix} = \begin{bmatrix} C_{ji} & 0 \\ 0 & F_{ji} \end{bmatrix}^{-1} \begin{bmatrix} D_{ji} & -(G_0 + G_1 \cos \omega t)E_{ji} \\ G_{ji} & H_{ji} \end{bmatrix} \begin{Bmatrix} a_i \\ b_i \end{Bmatrix}. \quad (17)$$

The coefficient matrices are defined by

$$\left. \begin{aligned} C_{ji} &= \int_{-1/2}^{1/2} \psi_j(D^2 - k^2)\psi_i dx = \langle \psi_j, (D^2 - k^2)\psi_i \rangle, \\ D_{ji} &= \langle \psi_j, (D^2 - k^2)^2\psi_i + ik\psi_j, [\psi_i D^2 W_0 - W_0(D^2 - k^2)\psi_i] \rangle, \\ E_{ji} &= \langle \psi_j, DT_i \rangle, \quad F_{ji} = \langle T_j, T_i \rangle, \\ G_{ji} &= \langle ikT_j, \psi_i \rangle, \quad H_{ji} = \langle T_j, \text{Pr}^{-1}(D^2 - k^2)T_i - ikT_j, W_0 T_i \rangle. \end{aligned} \right\} \quad (18)$$

All of these inner products are expressible in closed form.†

Equation (17) is a system of simultaneous ordinary differential equations for the amplitude functions $a_i(t)$ and $b_i(t)$ with periodic coefficients. According to Floquet theory (Yakubovich & Starzhinskii 1975; Joseph 1976), the solution vector $\phi(t)$ of such a system can be written as

$$\phi(t) = e^{\beta t} \Phi(t) \quad (19)$$

where β is complex and $\phi(t)$ is a vector periodic function with period $\tau = 2\pi/\omega$. The characteristic exponent β is given by

$$\beta = \frac{l}{\tau} \ln \mu \quad (20)$$

where μ is the eigenvalue of the Floquet transition matrix obtained by integrating (17) over the period τ with initial conditions given by the identity matrix.

To obtain the Floquet transition matrix, the $2N$ equations in (17) must be integrated $2N$ times over the period $\tau (= 2\pi/\omega)$ by numerical means. When the gravity modulation frequency ω is large, the time interval over which the integrations are performed is relatively small. As a consequence, the numerical integration is relatively time efficient and yields accurate results. But when ω is relatively small, the integrations become time consuming with deteriorating accuracy due to error accumulation. In this paper, we use the more efficient Chebyshev expansion method of Sinha & Wu (1991) to obtain the Floquet transition matrix. This method is explained in detail by Sinha & Wu, so only a brief summary is presented here. The amplitude functions, $a_i(t)$ and $b_i(t)$, and the periodic function, $\cos \omega t$, are each expanded into shifted Chebyshev polynomials of the first kind, $T_n^*(\hat{t})$, in the interval $0 \leq \hat{t} \leq 1$ where $\hat{t} = t/\tau$. The scalar product and the integrals of these polynomials can be expressed by the following recurrence relationships:

$$T_n^*(\hat{t})T_m^*(\hat{t}) = \frac{1}{2} [T_{n+m}^*(\hat{t}) + T_{|n-m|}^*(\hat{t})], \quad n, m = 0, 1, 2, \dots, \quad (21)$$

$$\int_0^{\hat{t}} T_n^*(\hat{t}) d\hat{t} = \begin{cases} [T_2^*(\hat{t}) - T_0^*(\hat{t})]/8, & n = 1 \\ \frac{1}{4} \left[\frac{T_{n+1}^*(\hat{t})}{n+1} - \frac{T_{n-1}^*(\hat{t})}{n-1} \right] - \frac{(-1)^n}{2(n^2-1)}, & n = 0, 2, 3, \dots \end{cases} \quad (22)$$

† The inner products are not listed in the paper because of their excessive length. Some of these are listed by Paliwal (1979). The rest are available on request to C. F. C.

As a result, the solution for the Floquet transition matrix becomes algebraic with no time integration needed. However, such a simplification is accompanied by the increased number of terms involved in the double expansion.

In order to obtain satisfactory convergence of the numerical procedure, we first determined the number of Galerkin terms needed to obtain satisfactory convergence (relative error $< 2.5 \times 10^{-4}$) under steady gravity. For the gravity modulation case, we used the same number of Galerkin terms, with a systematically increased number of Chebyshev terms, until satisfactory convergence was obtained. The number of Galerkin terms depends on Pr , while the number of Chebyshev terms depends on g_1/g_0 and ω , with more terms needed for large g_1/g_0 and small ω . The accuracy of the Chebyshev expansion method was checked by (a) comparing the critical Grashof number as the modulation amplitude ratio g_1/g_0 approaches zero to that for the steady gravity case and (b) comparing with the time integration method for $\omega \geq 100$. For a fluid with $Pr = 1.0$, using a 12-term Galerkin expansion, the steady gravity critical Grashof number, G_{0c} , is 7939.82 at the critical wavenumber $k_c = 2.81$. These values are slightly higher than the $G_{0c} = 7880$ and $k_c = 2.65$ found by Vest & Arpaci (1969), probably due to the larger number of terms used in our Galerkin expansion, but slightly lower than $G_{0c} = 8037.59$ and $k_c = 2.80$ found by Suslov & Paolucci (1995) using an integral Chebyshev collocation method. The values of G_{0c} and k_c calculated using the 12-term Galerkin expansion and the 14-term Chebyshev expansion for $\omega = 20$ at $g_1/g_0 = 0.02, 0.01, \text{ and } 0.005$ are:

g_1/g_0	k_c	G_{0c}
0.02	2.81	7940.15
0.01	2.81	7939.90
0.005	2.81	7939.84

In addition, we have compared the Chebyshev expansion method with the time integration procedure using a 12-term Galerkin expansion for $\omega \geq 100$ with $0.2 < g_1/g_0 < 1.4$. The results agree completely up to $g_1/g_0 = 0.8$ and within 0.25% for the rest. It is concluded that the Chebyshev expansion method is sufficiently accurate. We also found this method to be more efficient than the time-integration method for the frequency range considered, 20 to 1000.

4. Kinetic energy analysis

It is known that the instability under steady gravity is either shear driven or buoyancy driven, depending on whether the Prandtl number of the fluid is smaller or larger than 12.5, respectively. Suslov & Paolucci (1995)† examined the linear stability of natural convection of a non-Boussinesq flow with a low Prandtl number. The results show that, when ΔT is increased beyond the critical value, there is a sharp decrease in the critical Rayleigh number, accompanied by a sudden decrease of the critical wavenumber. A detailed analysis of the perturbation kinetic energy carried out by Suslov & Paolucci showed that the shear-driven instability at small ΔT became buoyancy driven as ΔT exceeded the critical value. It is of interest in the present problem to examine if additional gravitational forcing due to either an increase in the modulation amplitude, g_1 , or an increase in the modulation frequency is the cause of the observed mode switching. For this purpose, we examine all the terms that make

† We are indebted to the referee who brought this paper to our attention.

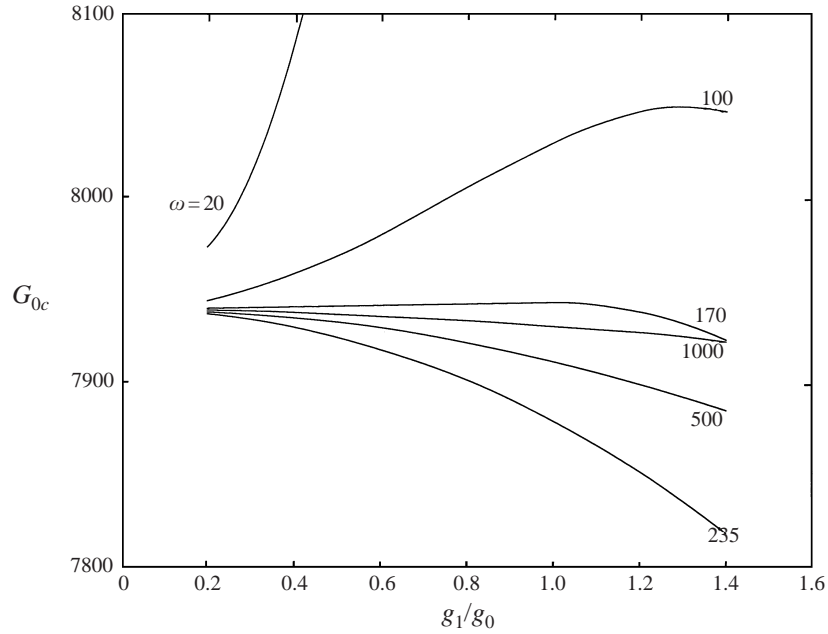


FIGURE 2. Effect of modulation amplitude ratio, g_1/g_0 , on the critical Grashof number, G_{0c} , for $Pr = 1$ at selected modulation frequencies, $\omega = 20, 100, 170, 235, 500$, and 1000 . All instabilities are in the synchronous mode.

up the substantial derivative of the perturbation kinetic energy:

$$\begin{aligned} \frac{d}{dt} \langle \frac{1}{2} (|u'|^2 + |w'|^2) \rangle &= \text{Re} \langle u'^* Dp' - ikw'^* p' \rangle - \text{Re} \langle w'^* u' DW_0 \rangle \\ &+ (G_0 + G_1 \cos \omega t) \text{Re} \langle w'^* T' \rangle - \{k^2 \langle |u'|^2 + |w'|^2 \rangle \\ &- \text{Re} \langle u'^* D^2 u' + w'^* D^2 w' \rangle \} \end{aligned} \quad (23)$$

in which $\langle \rangle$ denotes the mean across the slot, Re the real part, and $*$ the complex conjugate. Equation (23) shows that the rate of change of the perturbation kinetic energy is composed of four terms: the rate of work done by (a) the pressure gradient, (b) the mean shear, and (c) the buoyancy force; and the rate of dissipation, which is negative definite throughout the cycle. According to Floquet theory, the perturbation kinetic energy at the marginal state is a time-periodic function rather than a constant, as is the case for steady gravity. It is noted that u' , w' , and T' are the sums of their respective expansions, and the pressure gradient terms can be obtained using the momentum equations.

5. Results and discussion

5.1. $Pr = 1.0$

We first consider $Pr = 1.0$ since Baxi *et al.* (1974) presented results for the critical Grashof number for $\omega = 100, 500$, and 1000 . These will provide us with a basis for comparing our results. In figure 2, we present the critical Grashof number, G_{0c} , as a function of the modulation amplitude ratio, g_1/g_0 , for $\omega = 20, 100, 170, 235, 500$, and 1000 . Our results for $\omega = 100, 500$, and 1000 show the same characteristics as those

given by Baxi *et al.*, except that our values are slightly higher, again probably due to the larger number of Galerkin terms in our calculation. For these calculations, at $\omega = 20$, we used 12 Galerkin expansion terms and 20 Chebyshev terms; for $\omega \geq 100$, only 14 Chebyshev terms were needed to obtain convergence of the result. The results for $\omega = 20$ lie mostly out of the range of this graph. This will be discussed in more detail later.

For modulation frequencies $100 \leq \omega \leq 1000$, the critical states are all in the synchronous mode. For $\omega = 100$, the stability of the convection is slightly enhanced by gravity modulation within the amplitude ratios considered, $0.2 \leq g_1/g_0 \leq 1.4$. The maximum enhancement is obtained at $g_1/g_0 = 1.2$, with the value of G_{0c} increased by 1.4% over that for steady gravity. For $\omega = 170$, there is no discernible effect of gravity modulation on the stability of convection up to $g_1/g_0 = 1.0$. Beyond this amplitude ratio, G_{0c} is reduced slightly. At higher ω , the effect of modulation is destabilizing. The reduction of stability reaches its maximum value at $\omega = 235$. At $g_1/g_0 = 1.4$, the value of G_{0c} is reduced by 1.5% from that at steady gravity. For a range of ω from 230 to 250, the G_{0c} curves are very close to each other. When ω is increased beyond 250, the modulation effect becomes smaller, although it is still slightly destabilizing at $\omega = 1000$.

Jin & Chen (1997) found by numerical simulation of a tall, narrow tank with aspect ratio 20 that stability is considerably enhanced at $\omega = 25$ and $g_1/g_0 = 1$ for a $Pr = 1$ fluid. More specifically, they found that the critical Grashof number at steady gravity is 8800–8900. At $\omega = 25$, steady convection still prevailed at $G_0 = 10\,000$. To gain a better understanding of the phenomenon, we have studied the case of $\omega = 20$ in some detail. It is found that the marginal stability curve is bimodal, consisting of a synchronous and a subharmonic branch. For $g_1/g_0 \leq 0.8$, the instability is most critical in the synchronous mode. As $g_1/g_0 = 0.8$ is approached, the critical Grashof number of the subharmonic mode approaches that for the synchronous mode. This is shown in figure 3, in which the marginal stability curves (Grashof number G_0 vs. wavenumber k) for $g_1/g_0 = 0.78, 0.80, 0.81$, and 0.83 are presented. At $g_1/g_0 = 0.78$, figure 3(a), the synchronous mode with a larger wavenumber, k , is the more critical. As g_1/g_0 is increased to 0.80, figure 3(b), the critical Grashof number of the synchronous mode became slightly higher than that of the subharmonic mode. At $g_1/g_0 = 0.81$, figure 3(c), the difference between the two modes is clearly discernible, with the G_{0c} of the subharmonic mode -2.1% less than that for the synchronous mode. At $g_1/g_0 = 0.83$, figure 3(d), the difference between the two critical Grashof numbers becomes quite obvious. The variation of the critical Grashof number with amplitude ratio g_1/g_0 for $\omega = 20$ is shown in figure 4. The synchronous mode is shown by the solid line, and the subharmonic mode by the dotted line. As g_1/g_0 is increased from zero, there is a steady increase of G_{0c} from 7939 to a maximum value of 8913, at $g_1/g_0 = 0.8$, a 12.3% increase, which is comparable to the 13% increase reported by Jin & Chen. Beyond $g_1/g_0 = 0.8$, the subharmonic mode becomes the critical one, and G_{0c} decreases. At $g_1/g_0 \approx 0.92$, gravity modulation becomes destabilizing. The synchronous mode, after reaching a maximum critical Grashof number at $\sim 10\,700$, drops sharply and becomes the more critical mode at $g_1/g_0 \approx 1.3$. In figure 5, the critical wavenumber, k_c , shows abrupt changes at $g_1/g_0 = 0.8$ and 1.3 , where the mode switchings take place.

The result that the critical instability alternates between the synchronous and subharmonic modes as the modulation amplitude is increased at a constant frequency is quite similar to earlier results for convection in a horizontal fluid layer found by Gershuni *et al.* (1970), Gresho & Sani (1970), Saunders *et al.* (1992), and Terrones

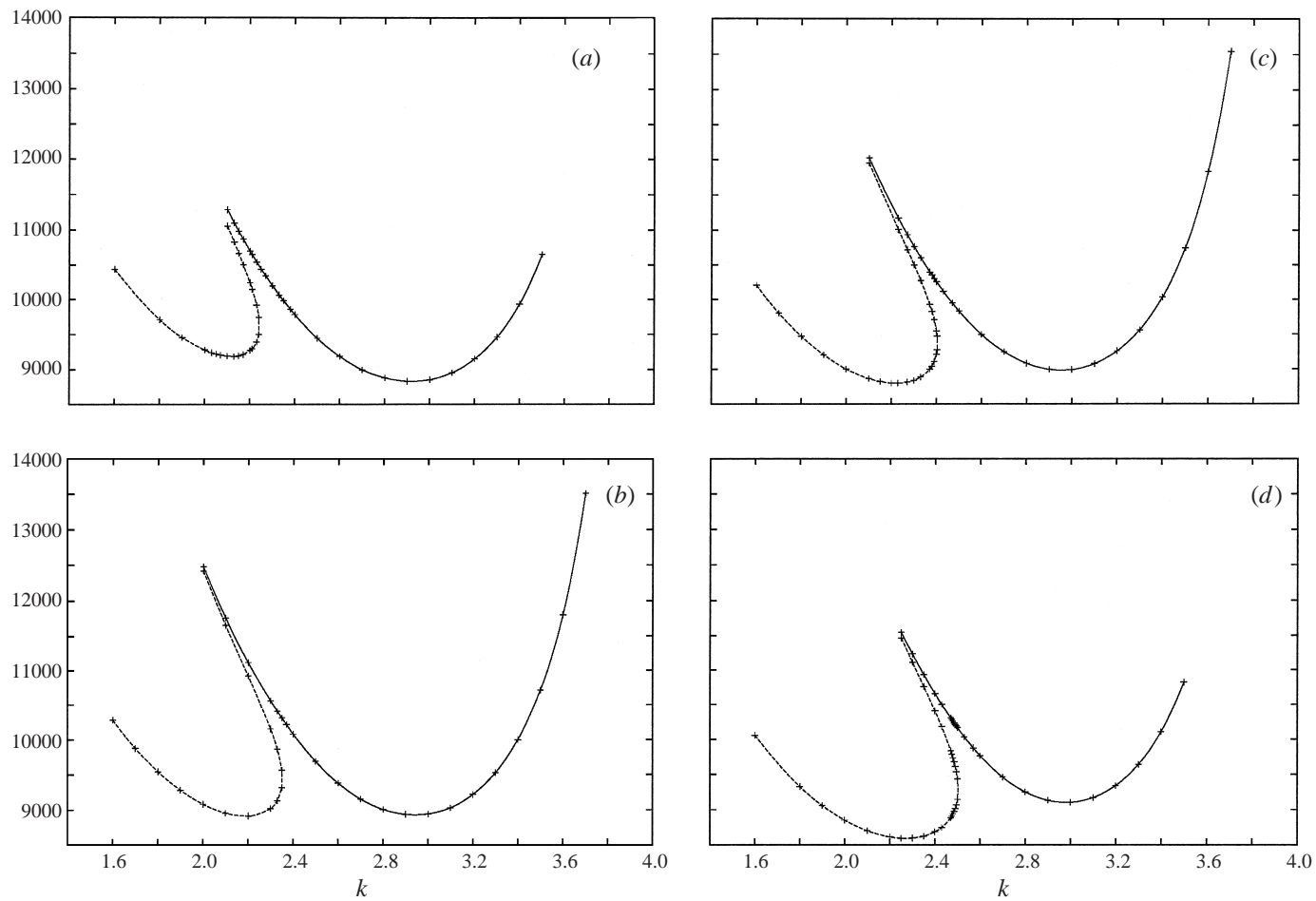


FIGURE 3. Marginal stability curves for $Pr = 1$ and $\omega = 20$ showing the competition between the synchronous (—) and subharmonic (- - -) modes. (a) $g_1/g_0 = 0.78$; (b) $g_1/g_0 = 0.80$; (c) $g_1/g_0 = 0.81$; (d) $g_1/g_0 = 0.83$.

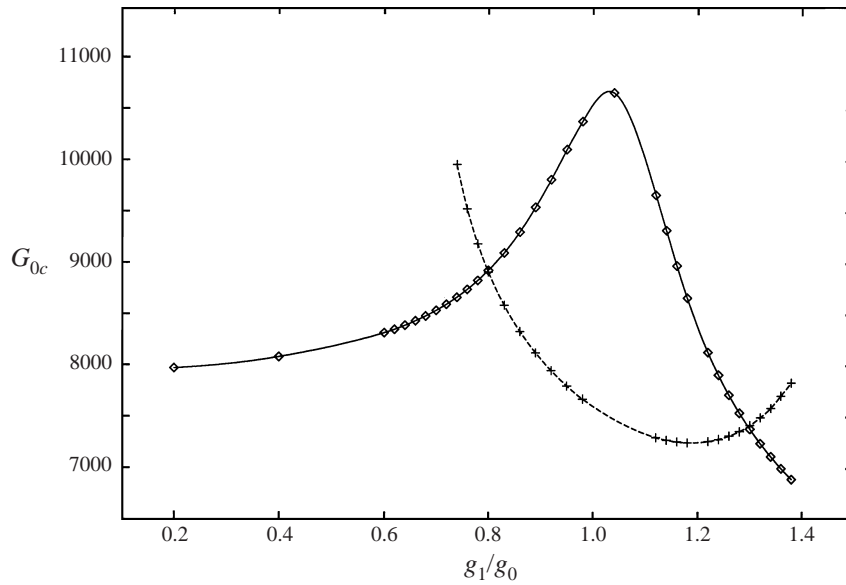


FIGURE 4. Variations of the critical Grashof number, G_{0c} , with modulation amplitude, g_1/g_0 , at $Pr = 1$ and $\omega = 20$. —, Synchronous mode; - - - -, subharmonic mode.

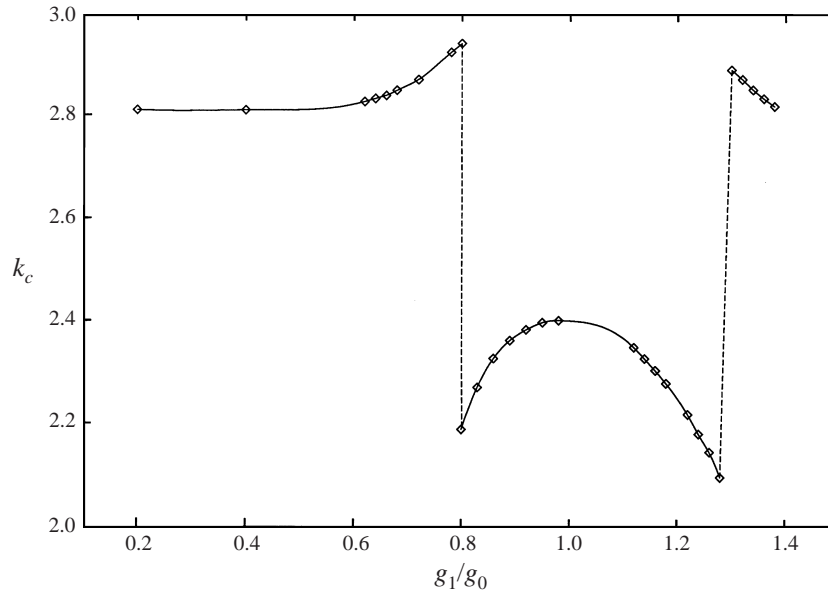


FIGURE 5. Variation of critical wavenumber, k_c , with modulation amplitude, g_1/g_0 , at $Pr = 1$ and $\omega = 20$. —, Synchronous mode; - - - -, subharmonic mode.

& Chen (1993). Stability equations for this type of problems can be reduced to the Mathieu equation, which has asymptotic stable solutions in either the synchronous or the subharmonic mode, depending on the modulation frequency and amplitude.

The results of Suslov & Paolucci (1995) suggest that mode switching of the instability can be caused by increased gravitational forcing (increasing ΔT in their problem). In order to determine whether the mode switching at $g_1/g_0 = 0.8$ in the present

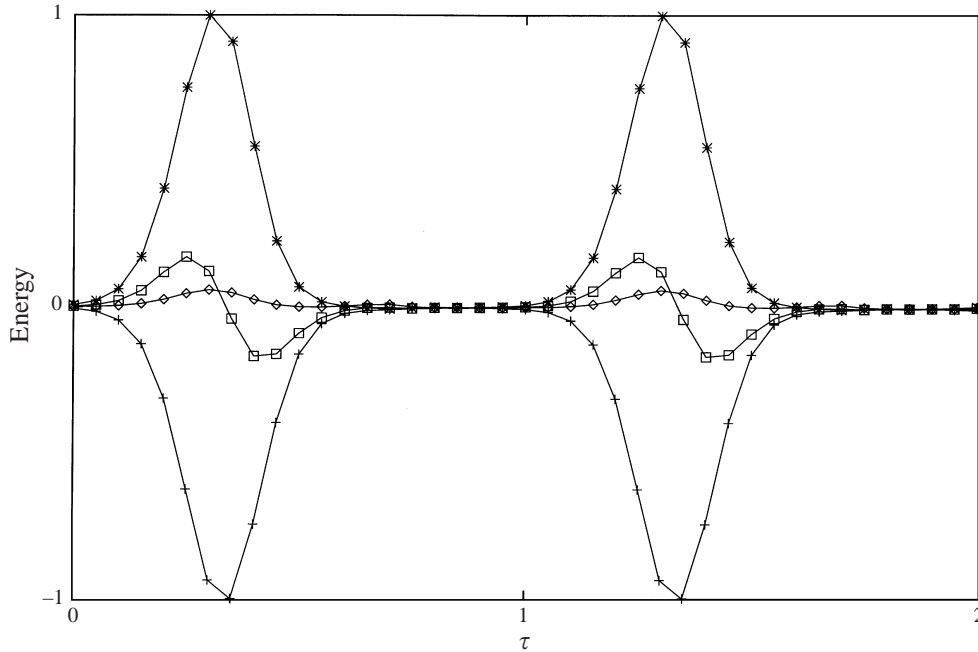


FIGURE 6. Contributions to the rate of change of perturbation kinetic energy at the marginal state for $Pr = 1.0$, $\omega = 20$, and $g_1/g_0 = 0.80$ in the subharmonic mode. *, shear; \diamond , buoyancy; +, dissipation; \square , $d/dt(KE)$. Results are shown for two modulation periods.

problem is caused by increased gravitational forcing or is a dynamical response to the modulation, we apply the perturbation kinetic energy analysis to the case of $Pr = 1$ shown in figure 3(b) in which the critical instability has just switched from the synchronous to the subharmonic mode at $g_1/g_0 = 0.8$. All the terms appearing on the right of (23) are calculated over two modulation periods and are plotted in figure 6 with all values normalized with respect to the maximum value in the shear work term. Rather than the work done by the pressure gradient, we present the time rate of change of the perturbation kinetic energy in figure 6. It is seen that there is active energy transfer from the mean shear to the instability during the first half of each cycle. Within the same time period, the buoyancy work is a small fraction of the shear work. The second half of the cycle is shown enlarged in figure 7, in which only shear and buoyancy work terms are shown. It is seen that, for approximately one-quarter of the cycle, buoyancy contributes more than shear to the perturbation kinetic energy. Averaged over one cycle, the ratio of buoyancy to shear contribution is 0.065, showing that the instability is certainly shear dominated. Calculations were also made for the case shown in figure 3(a) in which the instability is in the synchronous mode at $g_1/g_0 = 0.78$. Similar results were obtained, with shear work much larger than buoyancy work. For $Pr = 1$, the instability is shear driven, and the mode switching is a dynamical response to the gravity modulation.

5.2. $Pr = 25.0$

Under steady gravity, the marginal stability curve for the slot convection problem consists of two branches, the steady convection mode and oscillatory mode. For fluids with $Pr < 12.5$, the steady convection mode is the critical one and the critical Grashof number, G_{0c} , is a constant. But, for fluids with $Pr > 12.5$, the oscillatory mode is

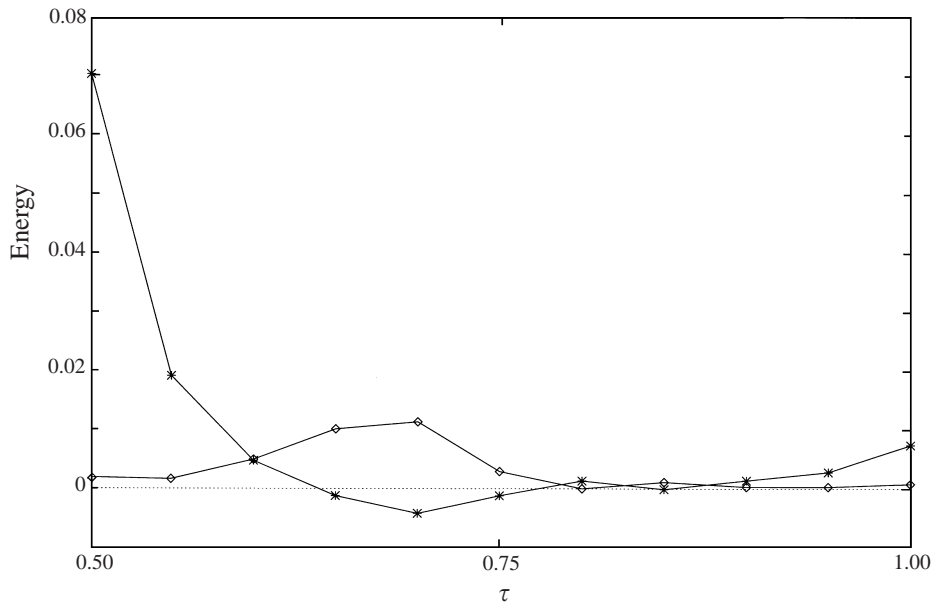


FIGURE 7. Enlarged view of contributions of shear (*) and buoyancy (◇) to the rate of change of perturbation kinetic energy for $\tau = 0.5$ to 1.0.

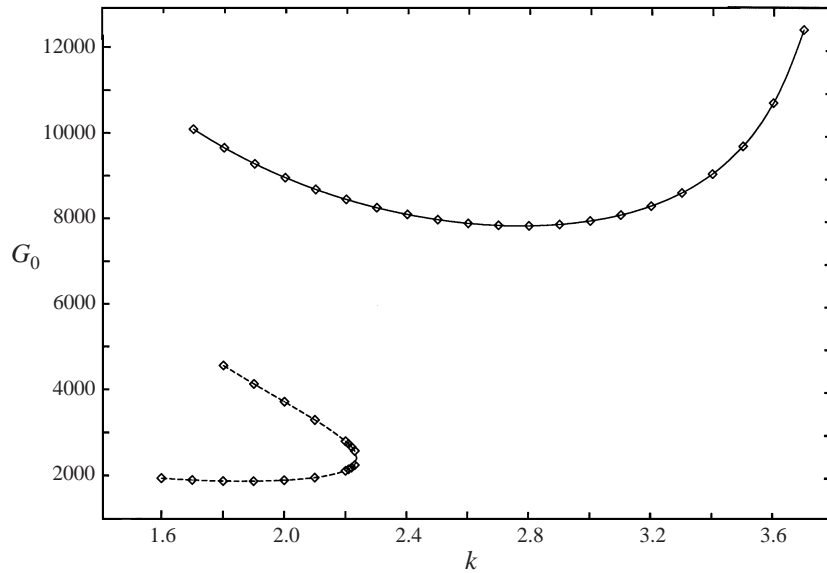


FIGURE 8. Marginal stability curve for $Pr = 25$ under steady gravity showing the steady convection branch (—) and the oscillatory branch (- - -).

the more critical one, with G_{0c} decreasing with increasing Pr (Chen & Pearlstein 1989). In figure 8, we show the marginal stability curve for $Pr = 25$, the case under consideration, with the steady convection mode indicated by a solid line and the oscillatory mode by a dashed line, which forms a lower detached branch of the marginal curve. The critical Grashof number $G_{0c} = 1888$, with a critical wavenumber, $k_c = 1.8$, oscillating at a critical frequency $\sigma_c = 27.2$.

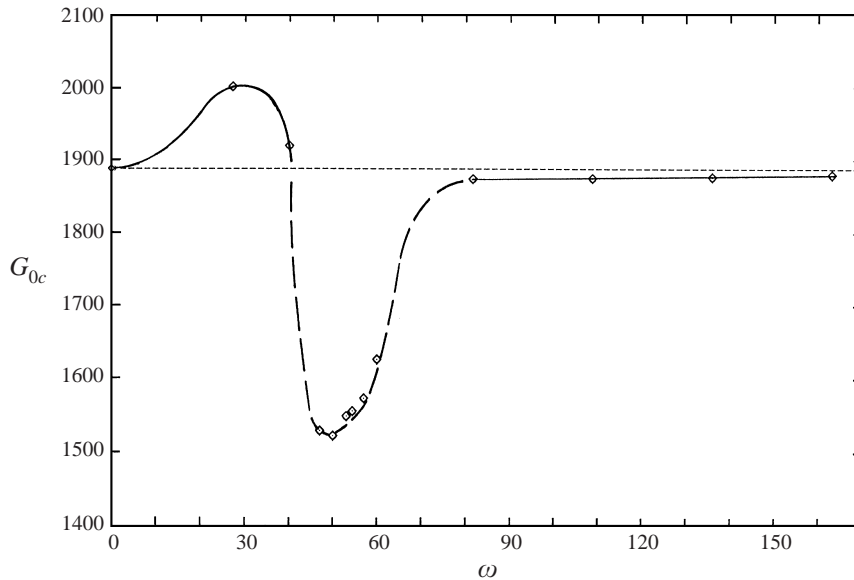


FIGURE 9. The critical Grashof number, G_{0c} , over a range of modulation frequencies, ω , for $Pr = 25$ at $g_1/g_0 = 0.5$. Note the resonant interaction in the frequency range $45 < \omega < 60$. —, Quasi-periodic mode; - - - -, subharmonic mode.

When the same vertical fluid layer is subjected to gravity modulation, the steady convection mode shown in figure 8 becomes the synchronous mode, with the fluid in each convection cell oscillating at the modulation frequency. The oscillating mode now becomes the quasi-periodic mode (Joseph 1976; Terrones & Chen 1993), in which the characteristic exponent β in (19) is the product of functions with incommensurate frequencies. As a result, any given wavenumber, there are two instability modes oscillating at incommensurate frequencies, whose sum is the modulation frequency. The quasi-periodic mode, similar to its counterpart the oscillatory mode under steady gravity, is generally the critical mode.

We study the possible resonance effect by calculating the critical state for a given amplitude ratio, but with modulating frequency, ω , varying 0 to 170, paying particular attention to $\omega = 27.2$ and its harmonics. These calculations were made with 30 Galerkin terms and 12 Chebyshev terms. For $g_1/g_0 = 0.1$, there is essentially no effect on the critical Grashof number throughout the forcing frequency range. At $g_1/g_0 = 0.5$, noticeable effects are found in the neighbourhood of $\omega = \sigma_c$ and $2\sigma_c$, as shown in figure 9. In this figure, the horizontal short-dashed line indicates the critical Grashof number under steady gravity, and the solid line represents the quasi-periodic mode. At $\omega = 27.2$, the stability is slightly enhanced by approximately 6%. In the neighbourhood of $\omega = 54.4 = 2\sigma_c$, however, the stability is greatly reduced, reaching a minimum value of $G_{0c} = 1523$ at $\omega = 50$, a 19% decrease from the steady gravity value. The instability is in the subharmonic mode indicated by a long dashed line. It is anticipated that as g_1/g_0 is increased from 0.5, the resonance effect will be increased, thus reducing stability further. The six critical points shown in the frequency range $45 < \omega < 60$ are all in the subharmonic mode, occurring on closed, detached branches of the marginal stability curves. Such a branch is shown for $\omega = 2\sigma_c = 54.4$ in figure 10. The detached subharmonic branch is at the lower

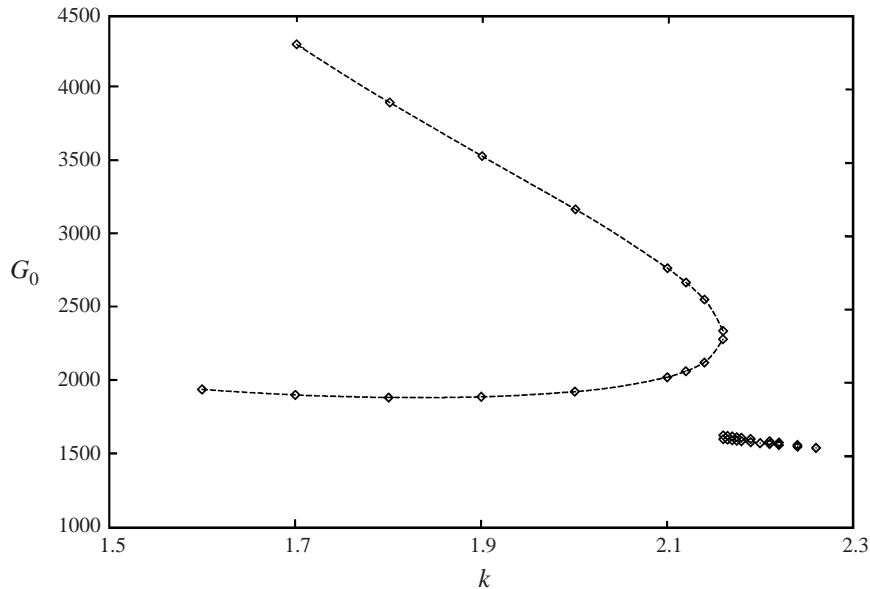


FIGURE 10. Marginal stability curve for $Pr = 25$ at $\omega = 54.4$ and $g_1/g_0 = 0.5$.
 -----, Quasi-periodic mode; detached subharmonic mode at lower right.

	ω	σ_1	σ_2
σ_c	27.2	26.44	0.76
$2\sigma_c$	54.4	27.20	27.20
$3\sigma_c$	81.6	26.31	55.29
$4\sigma_c$	108.8	27.69	81.11
$5\sigma_c$	136.0	27.73	108.27
$6\sigma_c$	163.2	27.77	135.43

TABLE 1. The values of σ_1 and σ_2 for $\omega = \sigma_c$ and its higher harmonics.

right. The wavenumber associated with the subharmonic branch is generally higher than that for the quasi-periodic branch.

The resonance effect occurring at $\omega \approx 2\sigma_c$ rather than at σ_c is due to the peculiar nature of the instability modes, which oscillate at two different frequencies. The values of σ_1 and σ_2 are listed in the table 1 for $\omega = \sigma_c$ and its higher harmonics. It is seen that one of the instability frequencies, say σ_1 , is always at a value near σ_c while $\sigma_2 = \omega - \sigma_1$. As ω approaches $2\sigma_c$, both wave are oscillating in the neighbourhood of σ_c , enabling the coupling of the forcing with the instability modes. Once the frequencies become equal, a resonance condition is attained, resulting in the reduction of stability, and the oscillation is in the subharmonic mode.

The results of the perturbation kinetic energy analysis for the resonant interaction case at $\omega = 54.4$ with $g/g_0 = 0.5$ are shown in figure 11, where all energy terms are normalized with respect to the maximum value of the buoyancy work term. In contrast to the $Pr = 1$ case shown in figure 6, active energy transfer occurs in 70% of the cycle. The buoyancy contribution to the perturbation kinetic energy overwhelms that of the shear. It is noted that, for approximately one-quarter of each cycle, the shear contribution is slightly larger than the buoyancy contribution. Averaged over

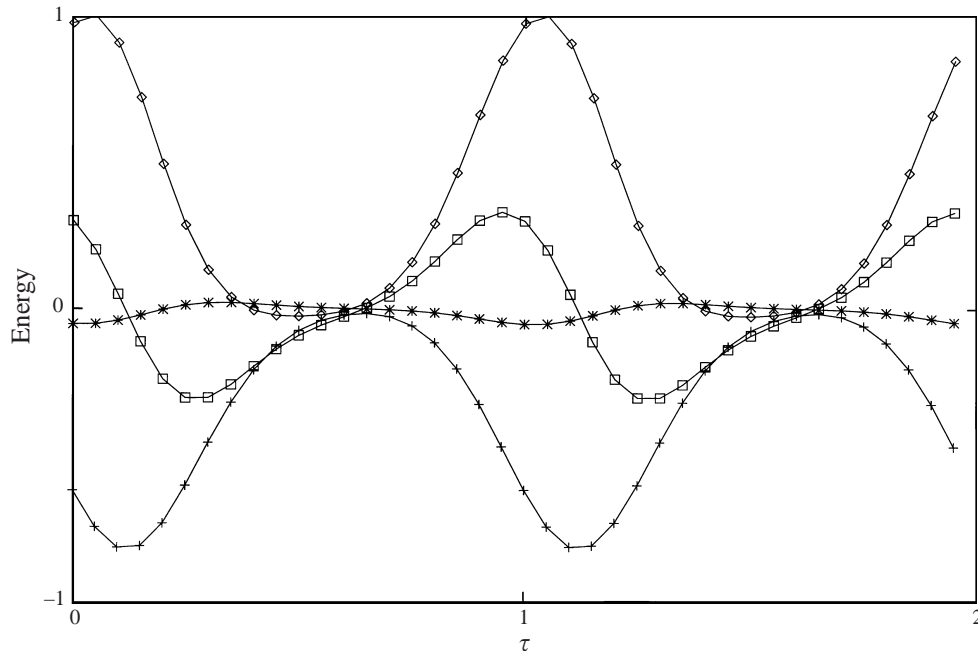


FIGURE 11. Contribution to the rate of change of perturbation kinetic energy at the marginal state for $Pr = 25$, $g_1/g_0 = 0.5$, and $\omega = 54.4$ at the resonance condition in the subharmonic mode. *, shear; \diamond , buoyancy; +, dissipation; \square , $d/dt(KE)$. Results are shown for two modulation periods.

one cycle, the ratio of shear to the buoyancy contribution is 0.027, exactly opposite to the $Pr = 1$ case, even though both instabilities are in the subharmonic mode. Calculations made for $\omega = 27.2$ and 81.6 (σ_c and $3\sigma_c$), for which the instability is the quasi-periodic mode, show that the averaged buoyancy-to-shear ratios are of the same order of magnitude as those for the resonance case.

6. Conclusions

We have examined the linear stability characteristics of natural convection of $Pr = 1$ and 25 fluids in an infinite slot under gravity modulation. For $Pr = 1$ and $\omega = 20$, analysis was carried out over a range of amplitude ratios, g_1/g_0 , from 0.2 to 1.4. At amplitude ratios < 0.8 , instability in the synchronous mode is the most critical. As the amplitude ratio is increased, the critical Grashof number for the subharmonic mode is decreasing and eventually becomes the critical mode at $g_1/g_0 = 0.8$. A reverse transition occurs at $g_1/g_0 = 1.3$, where the synchronous mode again becomes the critical one. Throughout the range of amplitude ratios studied, the stability is slightly enhanced as g_1/g_0 is increased from 0 to 0.92 and becomes slightly reduced thereafter. Analysis of contributions to the perturbation kinetic energy shows that, for $Pr = 1$, energy transfer from the mean shear is the dominant mechanism for instability regardless of its mode of oscillation, synchronous or subharmonic.

For $Pr = 25$, because the onset of instability under steady gravity is in the oscillatory mode, we searched for the possible effects of resonant interaction between the imposed gravity modulation and the oscillatory instability. Results show that, at $g_1/g_0 = 0.5$, resonance occurs in a subharmonic mode at $\omega \approx 2\sigma_c$, where σ_c is the frequency of oscillatory instability at steady gravity. The resonant interaction is

destabilizing, reducing the critical Grashof number by approximately 20%. Outside the resonant interaction zone, the instability is in the quasi-periodic mode consisting of two waves oscillating at incommensurate frequencies whose sum is the forcing frequency. Of the two waves, one is always oscillating near σ_c . When $\omega \approx 2\sigma_c$, both instability waves are oscillating at the same frequency, resulting in resonant interaction at the subharmonic mode.

Analysis of the perturbation kinetic energy shows that, for $Pr = 25$, the dominant mechanism for instability is buoyancy, regardless of its mode of oscillation, quasi-periodic or subharmonic. For both kinds of fluids, instability mode switching is a response to the periodic forcing and is independent of the dominant mechanism for instability.

More complicated interactions may be expected for fluids with Prandtl numbers near the transition value of 12.5. For these cases, the marginal stability curves may consist of all three branches, synchronous, subharmonic, and quasi-periodic, as in the case of horizontal double-diffusive fluid layers found by Saunders *et al.* (1992) and Terrones & Chen (1993). The instability characteristics of such fluids must be examined individually.

We thank Mr S. DeSilva for his help in determining the basic state and for the evaluation of some of the inner products. The financial support provided by the NASA Microgravity Science and Application Division through grant NAG3-1328 is gratefully acknowledged.

REFERENCES

- BAXI, C. B., ARPACI, V. S. & VEST, C. M. 1974 Stability of natural convection in an oscillating vertical slot. In *Proc. 1974 Heat Transfer and Fluid Mechanics Inst.* (ed. L. R. Davis & R. E. Wilson), pp. 171–183. Stanford University Press.
- BIRINGEN, S. & PELTIER, L. J. 1990 Numerical simulation of 3-D Bénard convection with gravity modulation. *Phys. Fluids* **5**, 754–764.
- CHANDRASEKHAR, S. 1961 *Hydrodynamic and Hydromagnetic Stability*. Oxford University Press.
- CHEN, C. F. & THANGAM, S. 1985 Convective stability of a variable-viscosity fluid in a vertical slot. *J. Fluid Mech.* **161**, 161–173.
- CHEN, Y.-M. & PEARLSTEIN, A. J. 1989 Stability of free-convection flows of variable-viscosity fluids in vertical and inclined slots. *J. Fluid Mech.* **198**, 513–541.
- FAROOQ, A. & HOMS, G. M. 1996 Linear and nonlinear dynamics of a differentially heated slot under gravity modulation. *J. Fluid Mech.* **313**, 1–38.
- GERSHUNI, G. Z. & ZHUKHOVITSKII, E. M. 1981 Convective instability of a fluid in a vibration field. *Izv. Akad. Nauk SSSR, Mekh. Zhidk. Gaza*, No. 4, pp. 12–19.
- GERSHUNI, G. Z., ZHUKHOVITSKII, E. M. & IURKOV, I. S. 1970 On convective stability in the presence of periodically varying parameter. *J. Appl. Math. Mech.* **34**, 442–452.
- GRESHO, P. M. & SANI, R. L. 1970 The effects of gravity modulation on the stability of a heated fluid layer. *J. Fluid Mech.* **40**, 783–806.
- HART, J. E. 1971 Stability of flow in a differentially heated inclined box. *J. Fluid Mech.* **47**, 547–576.
- JIN, Y. Y. & CHEN, C. F. 1997 Effect of gravity modulation on natural convection in a vertical slot. *Intl J. Heat Mass Transfer* **40**, 1411–1426.
- JOSEPH, D. D. 1976 *Stability of Fluid Motions I*, pp. 27–30. Springer.
- PALIWAL, R. C. 1979 Double-diffusive convective instability in an inclined fluid layer. PhD thesis. Rutgers University.
- SAUNDERS, B. V., MURRAY, B. T., MCFADDEN, G. B., CORIELL, S. R. & WHEELER, A. A. 1992 The effect of gravity modulation on thermosolutal convection in an infinite layer of fluid. *Phys. Fluids A* **4**, 1176–1189.
- SHARIFULIN, A. N. 1983 Stability of convective motion in a vertical layer in the presence of longitudinal vibration. *Izv. Akad. Nauk SSSR, Mekh. Zhidk. Gaza*, No. 2, pp. 186–188.

- SINHA, S. C. & WU, D.-H. 1991 An efficient computational scheme for the analysis of periodic systems. *J. Sound Vib.* **151**, 91–117.
- SUSLOV, S. A. & PAOLUCCI, S. 1995 Stability of natural convection flow in a tall vertical enclosure under non-Boussinesq conditions. *Intl J. Heat Mass Transfer* **38**, 2143–2157.
- TERRONES, G. & CHEN, C. F. 1993 Convective stability of gravity-modulated double cross-diffusive fluid layers. *J. Fluid Mech.* **255**, 301–321.
- THANGAM, S. & CHEN, C. F. 1986 Stability analysis on the convection of variable viscosity fluid in an infinite vertical slot. *Phys. Fluids* **29**, 1367–1372.
- VEST, C. M. & ARPACI, V. S. 1969 Stability of natural convection in a vertical slot. *J. Fluid Mech.* **36**, 1–15.
- YAKUBOVICH, V. A. & STARZHINSKII, V. M. 1975 *Linear Differential Equations with Periodic Coefficients*. John Wiley and Sons.